Proceedings World Geothermal Congress 2020
Reykjavik, Iceland, April 26 – May 2, 2020

Use of Cross g-functions to Calculate Interference between Ground Heat Exchangers used in Ground-source Heat Pump Systems

Matt S. Mitchell, Jeffrey D. Spitler and Signhild Gehlin

201 GAB, Oklahoma State University, Stillwater, OK 74078

spitler@okstate.edu

Keywords: Ground-source heat pump. Ground heat exchanger. Thermal interference. G-function. Cross g-function.

ABSTRACT

Ground-source heat pump systems are increasingly popular for providing single-family home heating in Nordic countries. As the density of installations increase, questions sometimes arise as to the influence of new systems on existing systems. These questions cannot be readily answered, as design and simulation techniques developed over the last 35 years have focused on analysis of individual systems without regard to the influences of other systems.

Response factor models of ground heat exchangers utilize pre-computed response functions known as g-functions. These g-functions give the response of the ground heat exchanger (non-dimensionalized temperature) to the past and current heat rejection or extraction of the ground heat exchanger. We might call this a "self-g-function."

In this paper, we define a "cross g-function" that gives the response of one ground heat exchanger to heat rejection or extraction of another ground heat exchanger. With this formulation, it is possible to determine the impact of a neighboring ground heat exchanger with a different load profile and history. This has many possible applications, but we demonstrate its use to study the sensitivity of nearby residential ground heat exchangers upon one another.

1. INTRODUCTION

Response function methods for analysis of ground heat exchangers used in ground-source heat pump systems were originally developed by Prof. Johan Claesson and his PhD student, Per Eskilson. (Claesson and Eskilson 1985, Eskilson 1987) These methods rely on spatial superposition to develop a response function for specific geometric arrangements of boreholes. The response function, known as a g-function, gives the borehole wall temperature due to a constant heat input rate:

$$T_b = T_g + \frac{q}{2\pi \mathrm{k}^*} \cdot g(t/t_s, r_b/H, B/H, D/H) \tag{1}$$

Time is non-dimensionalized against the time scale:

$$t_s = \frac{H^2}{9\alpha} \tag{2}$$

For design purposes, g-functions are often computed and compiled in libraries. Methods for computing g-functions are reviewed by Spitler and Bernier (2016); for recent improvements, see Cimmino (2018). Once the g-function has been calculated, temporal superposition is used to account for the present and past loads on the ground heat exchanger:

$$T_b = T_g + \sum_{i=1}^{n} \frac{(q_i - q_{i-1})}{2\pi \mathrm{k}^*} \cdot g((t_n - t_{i-1})/t_s, r_b/H, B/H, D/H) \tag{3}$$

Further details are given by Spitler and Bernier (2016). This elegant and computationally efficient solution has served well for design tools (Spitler 2000, BLOCON 2017) and simulation models. (Yavuzturk and Spitler 1999, Fisher et al. 2006) In all cases, the ground heat exchanger is assumed to operate without thermal interference from other ground heat exchangers. The ground heat exchanger (GHE) is assumed to be made up of a fixed number of boreholes, all of which serve the same heating and cooling loads.

However, as ground-source heat pump systems have become increasingly more popular, situations arise where it would be useful to be able to analyze the impact of one GHE upon other nearby GHE. Examples include:

- Determining the effect of nearby ground heat exchangers in densely packed urban environments. How will your neighbors' GHE affect your GHE? Witte (2018) has developed a simplified graphical method for use in The Netherlands based on line-source theory. Fascì et al. (2018) investigates the effects of load averaging and temporal resolution of thermal loads for interfering GHE systems. Fascì and Lazzarotto (2019) propose a method to evaluate the effects of densely packed boreholes on the borehole temperature using a stacked finite line-source model (Cimmino and Bernier 2014).
- When an existing GHE is insufficient to meet the building loads, whether due to a poor initial design or changes in the building loads, adding additional boreholes may be the best solution. In this case, the borehole configuration changes with time and a practical analysis approach is to treat the old GHE and the new portion of the GHE as separate GHEs serving the same load, but with different start dates.
- Yu et al. (2017) have proposed zoning of the ground heat exchanger for cooling-dominated buildings that have a high ratio of heat rejected to heat extracted. By only operating the perimeter boreholes in the cooling season, the excess heat rejected

to the ground is more effectively dissipated. The ability to model the two separate zones of the GHE as separate GHEs with different load schedules would facilitate design of such systems.

Therefore, the objectives of this paper include definition of a "cross" g-function that gives the temperature response of one GHE to another GHE, presentation of a method for calculating the cross-g-function, validation of the method, and application of the methodology to examine the densely-packed residential GHE problem.

2. DEFINITIONS

First, where confusion may arise, we will call the original g-functions defined in Equation 1, the "self-g-function" and may use the conventional nomenclature (a "g" without subscripts). For sake of clarity, since it is possible that there will be more than two GHE, self-g-functions may be notated as $g_{A\to A}$ for the effect of GHE *A* on GHE *A*. The cross-g-function giving the temperature impact of GHE *B* on GHE *A* will be designated $g_{B\to A}$. The original definition of the self-g-function utilizes a non-dimensional time as shown in Equation 2 – using the average, active depth of the self-boreholes and the soil's thermal diffusivity. We will assume here that the soil diffusivity is the same for all GHE being analyzed, but the active depth of the two GHE may well be different. The original definition of the self-g-function is implicitly a non-dimensional temperature change. Rearranging Equation 1:

$$g((t_n - t_{i-1})/t_s, r_b/H, X_b/H, D/H) = \frac{(T_b - T_g)(2\pi k^*)}{q} \tag{4}$$

This form requires the heat pulse, q, to represent the heat input per unit length of ground heat exchanger. Non-dimensionalization of the temperature rise and time when two different ground heat exchangers are involved may no longer be as useful as it was for self-g-functions. At present, we do not anticipate creating libraries of cross g-functions, though it might be useful for the residential interference problem. In such a case, the cross g-function might become a function of the depth ratio of the two heat exchangers. Furthermore, for the cross g-function, we do not anticipate the r_b/H of the nearby GHE to be important. Nevertheless, for computational convenience, we retain the non-dimensionalization as follows:

$$g_{B\to A}\big((t_n - t_{i-1})/t_{s,A}\big) = \frac{(T_{b,A} - T_g)(2\pi k^*)}{q_B} \tag{5}$$

It should be understood that $g_{B\to A}$ is computed for the specific geometries of GHEs *A* and *B*, and no attempt is being made to generalize them to other geometry/size combinations. As can be seen in Equation 5, the time scale is for the GHE *A* and the heat input pulse is applied to GHE *B*. Then, for a case where there are two GHEs, *B* and *A,* the borehole wall temperature for GHE *A* can be computed as:

$$\begin{aligned} T_{b,A} = T_g &+ \sum_{i=1}^{n} \frac{(q_{A,i} - q_{A,i-1})}{2\pi \mathrm{k}^*} \cdot g_{A\to A}\big((t_n - t_{i-1})/t_{s,A}, r_b/H, X_b/H, D/H\big) \\ &+ \sum_{i=1}^{n} \frac{(q_{B,i} - q_{B,i-1})}{2\pi \mathrm{k}^*} \cdot g_{B\to A}\big((t_n - t_{i-1})/t_{s,A}\big) \end{aligned} \tag{6}$$

If there are more GHE, the second row of Equation 6 could be placed in a summation covering GHEs *C, D, E*, etc.

3. METHODOLOGY FOR CALCULATING CROSS G-FUNCTIONS

Several methods have been developed for calculating self-g-functions. These methods have evolved to be able to use different mathematical modeling techniques for better accuracy and computation speed. The methods have also evolved to be able to handle different approximations for the borehole wall condition. Cimmino (2018) performs a thorough review of these methods and are therefore not discussed here.

The methods used here to compute the self- and cross-g-functions is based on the work by Marcotte and Pasquier (2009), which discretizes each borehole into a series of point-sources. The point-to-point response from each point to all other points is then determined, which gives the average borehole wall temperature response of the GHE. The model assumes a uniform heat flux borehole wall boundary condition and the soil temperature and properties are constant spatially and temporally. The average borehole wall temperature is computed as shown in Equation 7.

$$\Delta T_W(t) = \sum_{i=1}^{N} \frac{H_i}{H_{tot}} \sum_{j=1}^{N} \Delta T_{j\to i}(t) \tag{7}$$

The average borehole wall temperature change of borehole i caused by heat transfer from borehole j is shown in Equation 8.

$$\Delta T_{j\to i}(t) = \frac{q_j}{4\pi k H_i} \left(\int_{u_1^i}^{u_2^i} \int_{u_1^j}^{u_2^j} \frac{\mathrm{erfc}\left(\frac{d(u_i, u_j)}{2\sqrt{\alpha t}}\right)}{d(u_i, u_j)} - \frac{\mathrm{erfc}\left(\frac{d(u_i, u_j')}{2\sqrt{\alpha t}}\right)}{d(u_i, u_j')} du\, du' \right) \tag{8}$$

Where:

$$u_n = (x_n, y_n, z_m) \tag{9}$$

$$u'_n = (x'_n, y'_n, z'_n) \tag{10}$$

$$d(u_i, u_j) = \sqrt{(x_i - x_j)^2 + (y_i - y_j)^2 + (z_i - z_j)^2} \tag{11}$$

$$d(u_i, u'_j) = \sqrt{(x_i - x'_j)^2 + (y_i - y'_j)^2 + (z_i - z'_j)^2} \tag{12}$$

In order to account for the semi-infinite ground, each borehole is also mirrored about the ground surface to generate an imaginary borehole which has the opposite heat flux. Combining Equations 4, 7, and 8, g-functions can be computed as shown in Equation 13.

$$g = \frac{1}{2H_{tot}} \sum_{i=1}^{N} \sum_{j=1}^{N} \left(\int_{u_1^i}^{u_2^i} \int_{u_1^j}^{u_2^j} \frac{\operatorname{erfc}\left(\frac{d(u_i, u_j)}{2\sqrt{\alpha t}}\right)}{d(u_i, u_j)} - \frac{\operatorname{erfc}\left(\frac{d(u_i, u'_j)}{2\sqrt{\alpha t}}\right)}{d(u_i, u'_j)} du\, du' \right) \tag{13}$$

As applied to the computation of self- and cross-g-functions, this can be seen in Equations 14 and 15, respectively. $N_{b,A}$ represents the number of boreholes in GHE A, and $N_{b,B}$ represents the number of boreholes in GHE B.

$$g_{A \to A} = \frac{1}{2H_{A,tot}} \sum_{i=1}^{N_{b,A}} \sum_{j=1}^{N_{b,A}} \left(\int_{u_1^i}^{u_2^i} \int_{u_1^j}^{u_2^j} \frac{\operatorname{erfc}\left(\frac{d(u_i, u_j)}{2\sqrt{\alpha t}}\right)}{d(u_i, u_j)} - \frac{\operatorname{erfc}\left(\frac{d(u_i, u'_j)}{2\sqrt{\alpha t}}\right)}{d(u_i, u'_j)} du\, du' \right) \tag{14}$$

$$g_{B \to A} = \frac{1}{2H_{A,tot}} \sum_{i=1}^{N_{b,A}} \sum_{j=1}^{N_{b,B}} \left(\int_{u_1^i}^{u_2^i} \int_{u_1^j}^{u_2^j} \frac{\operatorname{erfc}\left(\frac{d(u_i, u_j)}{2\sqrt{\alpha t}}\right)}{d(u_i, u_j)} - \frac{\operatorname{erfc}\left(\frac{d(u_i, u'_j)}{2\sqrt{\alpha t}}\right)}{d(u_i, u'_j)} du\, du' \right) \tag{15}$$

Numerical integration has been performed using Simpson's formula (Moin 2010). Also, keep in mind that the time scale for the self- and cross-g-functions are based on the average length of boreholes in GHE A as is shown in Equation 16.

$$t_{s,A} = \frac{H_{A,ave}^2}{9\alpha_s} \tag{16}$$

4. VALIDATION

The cross g-functions have been validated by comparing a number of cases that could be calculated with self g-functions, then subdividing the borehole field into two or more smaller borehole fields, and applying the same loads at the same time. With these restrictions (same load, same start time), the net effect should be the same whether it is treated as one borehole field or two. For example, the borehole field shown in Figure 1 can be treated as a single borehole field, “C”, or as two borehole fields, “A” and “B”.

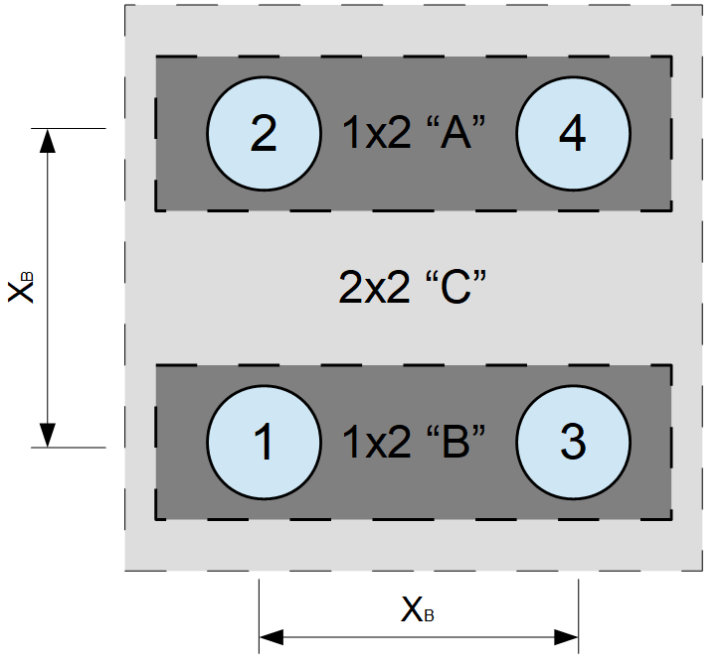

Figure 1: Example borehole fields A, B, and C used for validation

The self g-function for field “C” should be the same as the sum of the self g-function for A and the cross g-function, $g_{B\to A}$. As can be seen in Figure 2, this is the case. Further details and additional validation cases may be found in Mitchell (2019).

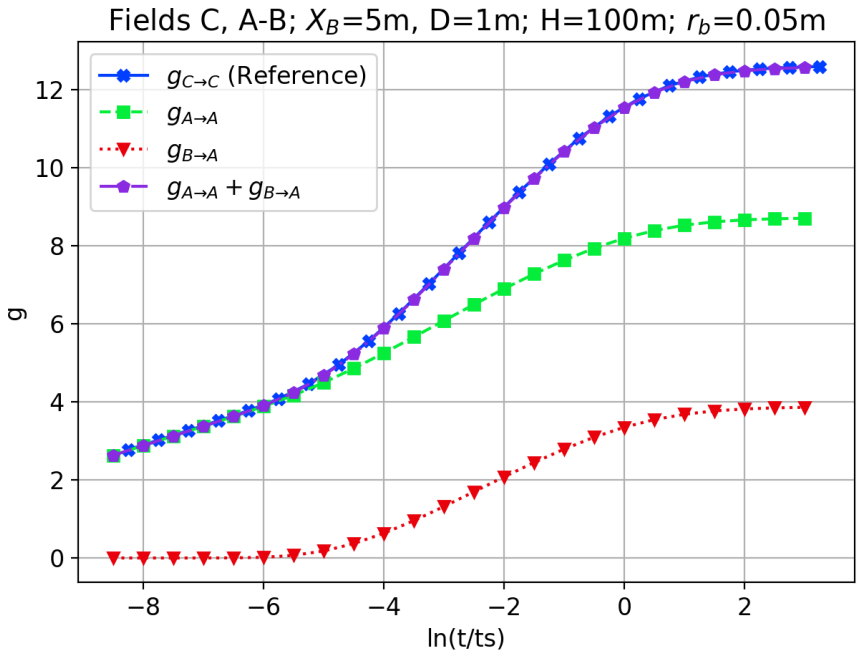

Figure 2: Self- and cross-g-functions for GHE A, B, and C validated against reference methods

5. APPLICATION

For example purposes, a typical Swedish single-family house – a renovated 1940s-era house with 125 sq. m. floor area in Stockholm is utilized (Gehlin and Spitler 2014). Hourly building heating loads for a typical Stockholm meteorological year were estimated with EnergyPlus. Figure 3 shows the house heating loads and outdoor air temperature. Hourly domestic hot water heating loads (Figure 4) are based on actual measured data for a Swedish household (Nordman 2014).

The heat pump is a typical residential water-to-water ground source heat pump used in Scandinavia. It incorporates an integrated hot water storage tank as shown in Figure 5. The heat pump capacity is 7 kW; loads in excess of this are met by an electric-resistance immersion heater which has a capacity of 7 kW. The heat pump operation and model are described in detail by Gehlin and Spitler (2014).

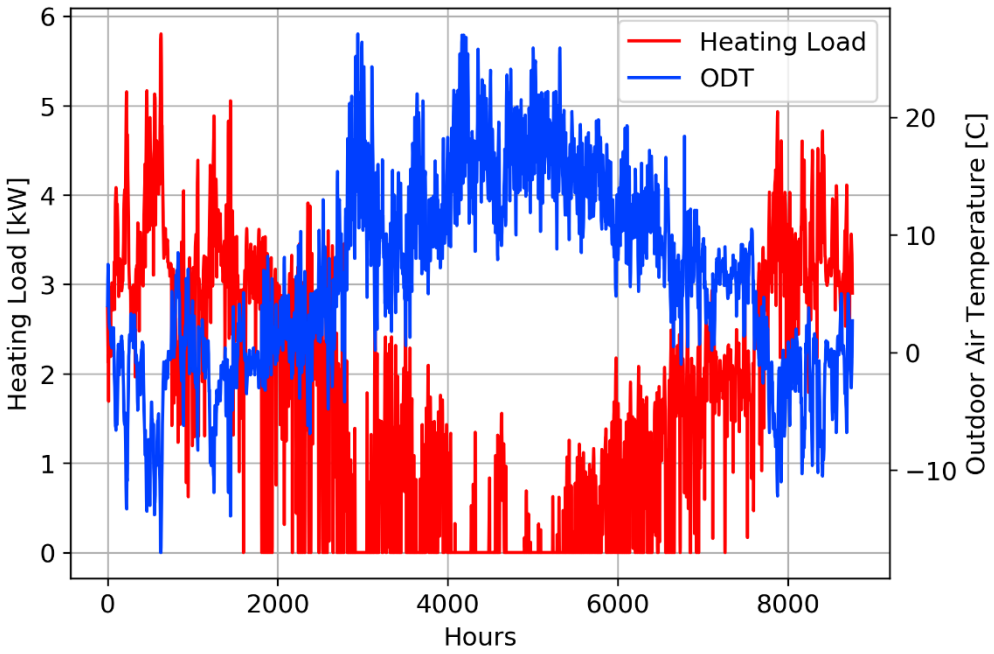

Figure 3: Heating load and outdoor air temperature

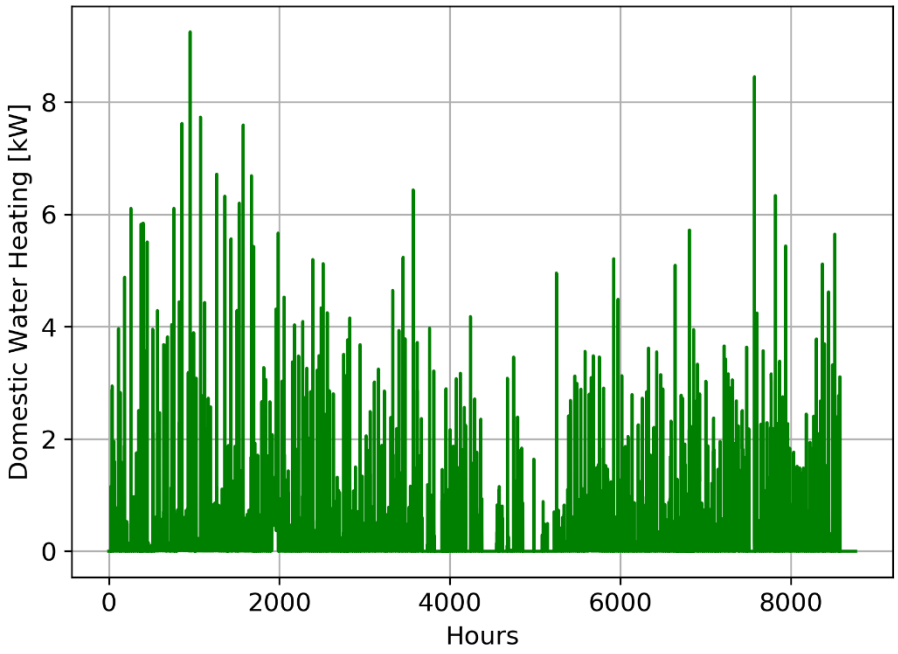

Figure 4: Domestic hot water heating loads

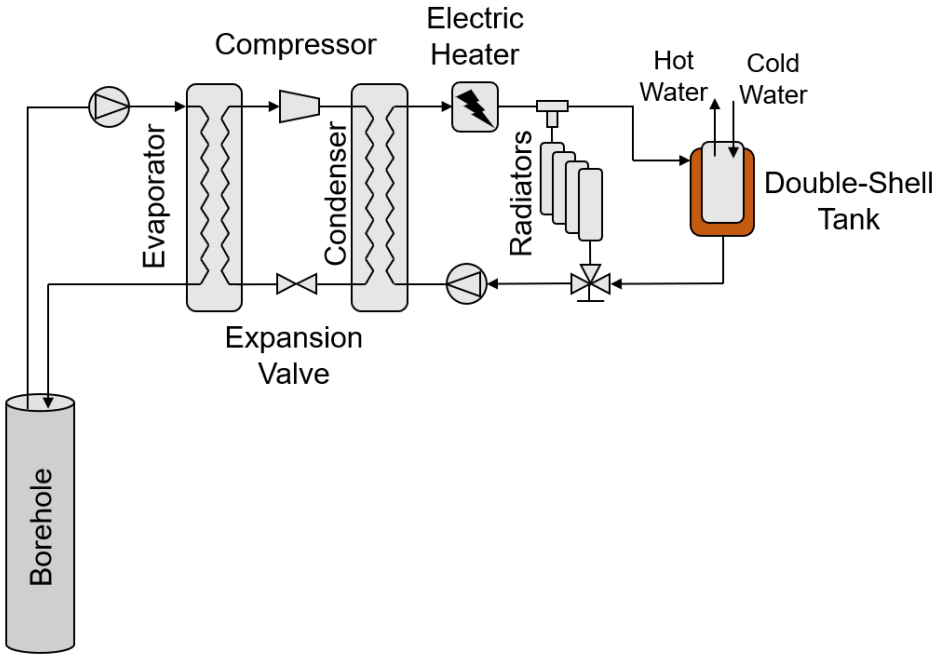

Figure 5: Ground-source heat pump system

The ground heat exchanger model used is similar to the response factor model given originally by Eskilson and Claesson (1988), with the model having been extended to account for neighboring GHE effects. Additional details regarding the model can be found in Mitchell (2019).

Borehole and soil parameters are given in Table 1 and are based on parameters for a typical Swedish borehole. Soil properties were set based on data provided by Spitler et al. (2014). Swedish boreholes are generally water filled boreholes, so the grout heat capacity was set to be equal to that of water, and the grout thermal conductivity was set to give a borehole thermal resistance of approximately 0.07 K/(W/m) which is a typical value (Gustafsson and Gehlin 2008). A 25% by mass ethanol-water antifreeze mixture was used and the flow rate was set to give a Reynolds number of approximately 6000 at 20°C.

Table 1: Borehole configuration parameters

Soil Conductivity	3.5 W/m-K
Soil Heat Capacity	2.678 MJ/m^3-K
Grout Conductivity (adjusted to give $R_b \approx$ 0.07 K/(W/m))	3.5 W/m-K
Grout Heat Capacity	4.2 MJ/m^3-K
Borehole Diameter	114 mm
Borehole Length	150 m
Pipe Outer Diameter	40 mm
Pipe Inner Diameter	34.9 mm
Pipe Conductivity	0.39 W/m-K
Pipe Heat Capacity	1.8 MJ/m^3-K
Shank Spacing	51.3 mm
Mass Flow Rate	0.446 kg/s

For purposes of example, the house was first analyzed with no neighboring boreholes by performing an hourly simulation for 20 years using the heat pump and ground heat exchanger models described previously. Figure 6 shows the heat pump inlet temperature for the 20-year simulation. The hourly, average monthly and average annual temperatures are shown. As is expected for a heating-dominated system, the average temperature decreases over the course of the 20-year simulation. The average annual heat pump inlet temperature decreases by about 0.8°C over the 20 years.

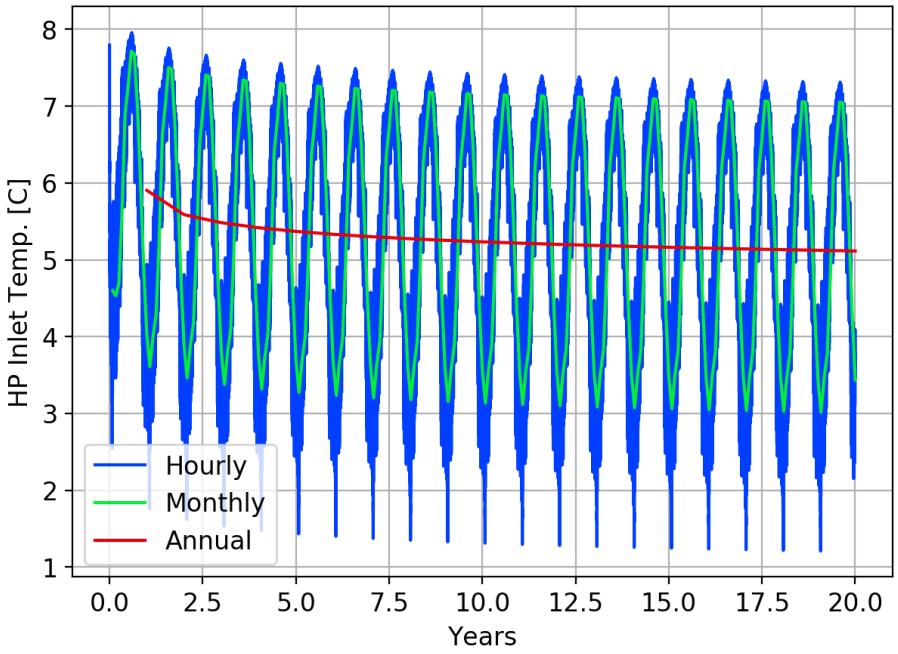

Figure 6: Heat pump inlet temperature for single system

This system with no neighboring GSHP systems and no neighboring ground heat exchanger (GHE) will be referred to as the "lone system". Next, the effects of a single neighboring system with a borehole at various distances away from the lone system borehole are considered. The neighboring borehole is placed at distances of 10, 15, and 20 m away from the lone borehole. The neighboring house and system are assumed to be identical to the lone system, and the GHE loads for the neighboring system are taken from the first year of operation of the lone system. These loads are repeated each year of the simulation and the effects of the lone system on the neighboring system are not considered. As a result, this is expected to be a worst-case scenario since the neighboring system will be affected by the lone system, with the decreased temperatures resulting in less heat extraction and more immersion heater use. As before, an hourly simulation was performed for 20 years while applying the building and domestic hot water loads given for the lone system, and also now considering the effects of the neighboring systems.

Figure 7 shows the average annual heat pump inlet temperature and the temperature difference from the lone system case, which was shown previously in Figure 6. From this we can see that the additional degradation in average heat pump inlet temperature when the neighboring system effects are considered. For the neighboring borehole located at 10 m away from the lone system borehole, the annual heat pump inlet temperature drops by over 1.3°C vs. the 0.8°C decrease when no neighboring system effects are considered. For the systems spaced at 15 and 20 m, the inlet temperature degradation is approximately 1.2 and 1.1°C, respectively.

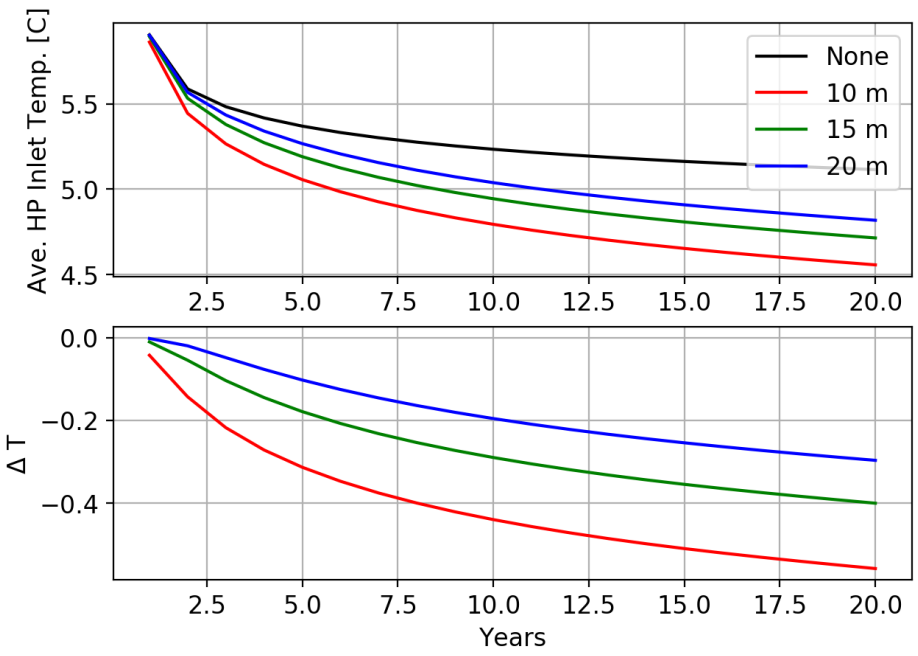

Figure 7: Average annual heat pump inlet temperature including neighboring system effects

Lower heat pump inlet temperatures leads to lower heat pump capacity and lower heat pump COP. For a heating-only application, this leads to more of the heating load being satisfied by the compressor energy and immersion heating. Less energy is then being extracted from the ground heat exchanger. This is shown below in Figure 8 where the annual heat pump coefficient of performance (COP) is plotted for the 20-year simulation.

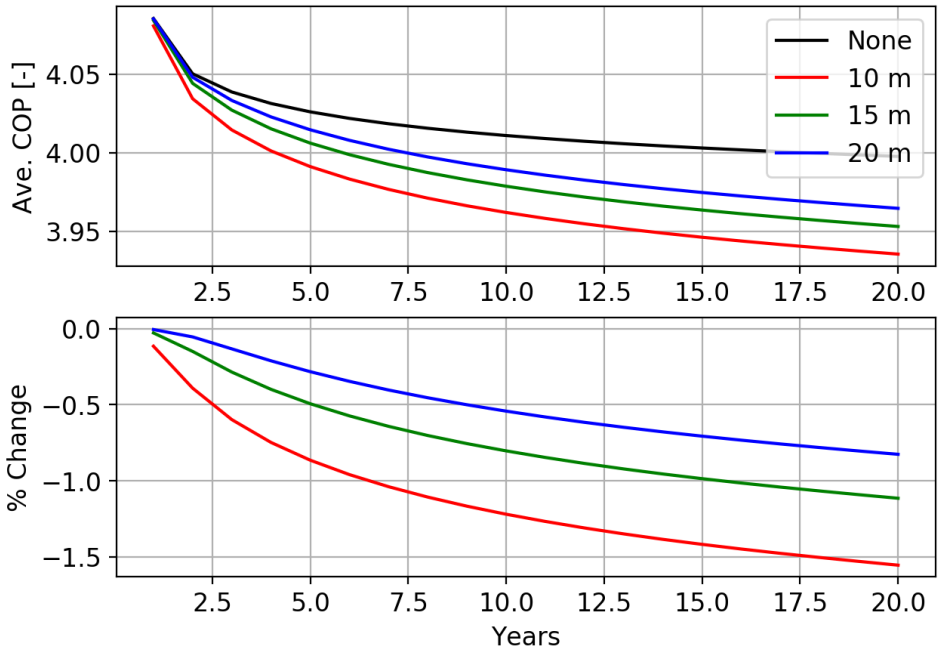

Figure 8: Average annual heat pump COP

Over the course of the 20-year simulation, we can see that for the 10 m neighbor-case the COP decreases by approximately 1.5% beyond the decrease already present for the no-neighbor-system case where no neighboring effects are considered. Note that the percent change data indicated in the figure are referenced from the lone system case for each simulation year. For the 15 m and 20 m cases, the heat pump COP degrades by about 1.1% and 0.8%, respectively.

Note that for heating-dominated situations such as this, the decrease in heat pump performance due to lower source-side entering fluid temperatures results in less energy being extracted from the soil and more heating energy being provided from the compressor. The decrease in heat pump capacity due to lower source-side entering fluid temperatures results in more heating energy being provided by the immersion heater. The decreased heat extraction may have a self-balancing effect that will allow the systems to continue to operate longer than would occur if the loads were cooling dominated. For a cooling-dominated load, the resulting decrease in heat pump performance will result in more energy being rejected to the soil. This in turn leads to further degradation of the heat pump performance. This situation is not expected to be self-balancing.

Figure 9 shows the total electrical energy used by the backup electrical immersion heater. Over the course of the 20-year simulation, we can see that immersion heater electrical energy used for the 10 m neighbor case increases by about 12% over the no-neighbor-system case. The 15 and 20 m cases result in about 8% and 6% increases, respectively. However, in this case the electric backup heater uses a relatively small percentage of the total electrical energy.

Comparing the 20th year of operation for the 10 m spacing case to the no-neighbor case, the compressor electricity increases by about 1.6% or 68.8 kWh, while the immersion heater electricity increases by 11.4% or 13.3 kWh. So, the decreased heat pump performance has a more significant effect, by about a factor of 5, than the decreased heat pump capacity.

Figure 10 shows the total electrical energy used by both the heat pump and the backup electrical heater. For the 10 m neighbor system case, an additional 1.9% electrical energy is used each year at the end of the 20 years. For the 15 m and 20 m neighbor cases, the total energy usage increase by about 1.3 and 1%, respectively.

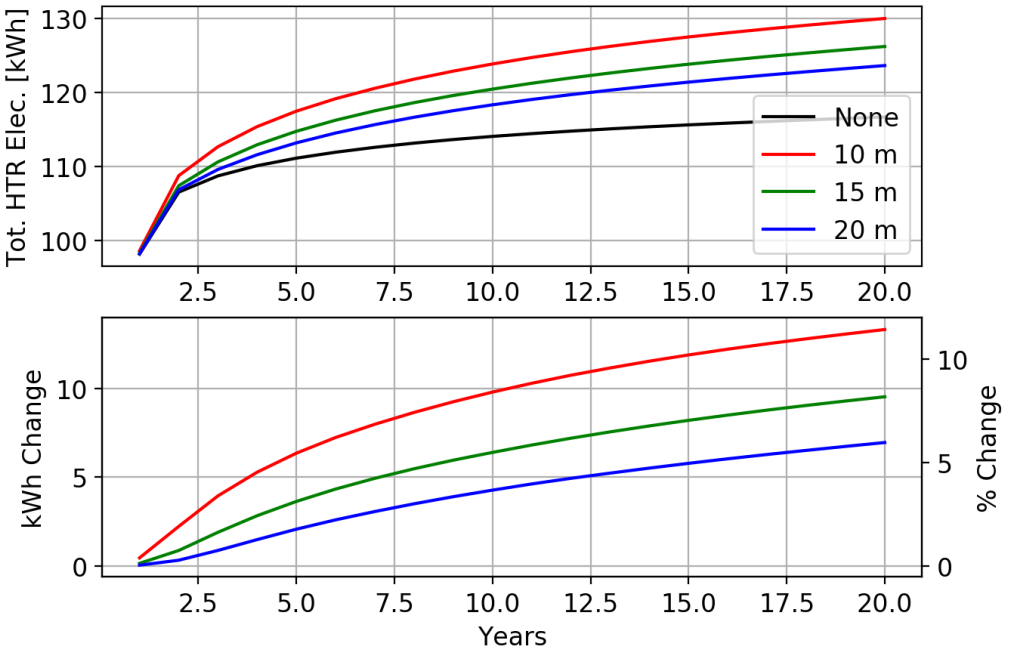

Figure 9: Annual electrical immersion heater energy usage

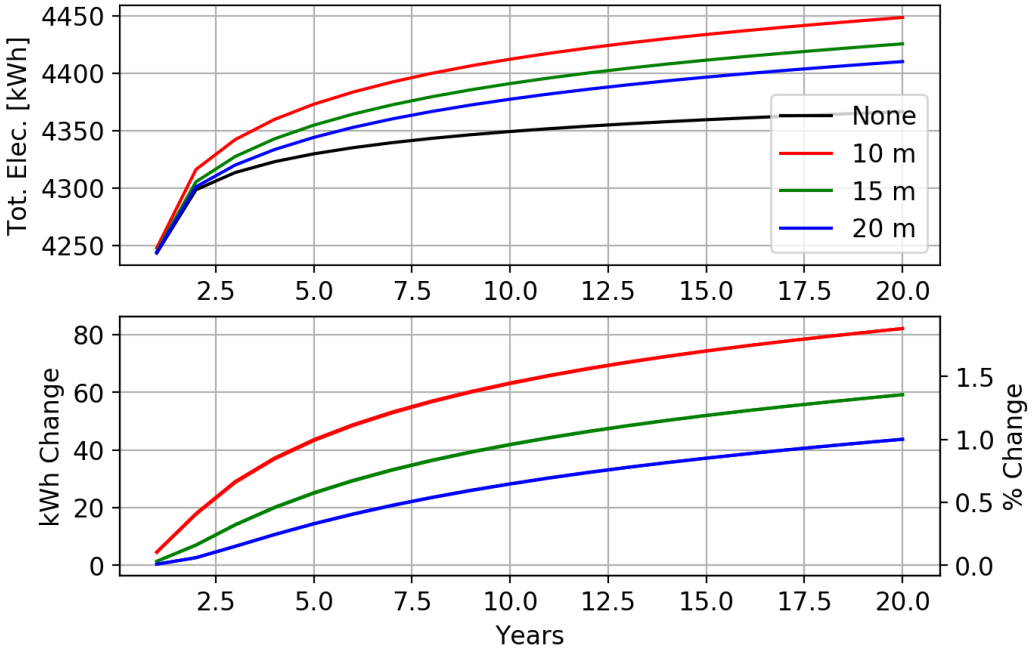

Figure 10: Total heat pump and immersion heat electrical energy

6. CONCLUSIONS AND RECOMMENDATIONS

This work has defined the concept of cross-g-functions and described how they are computed. A brief validation of the method is given and a study is performed describing how the method is applied and used to examine the densely-packed residential GHE problem. System loads, a heat pump model, and the GHE are described. Finally, the study is performed by comparing the energy usage for a lone system with no neighboring boreholes to a system with a single neighboring borehole, with the borehole-to-borehole spacing ranging between 10 and 20 m. A single neighboring system, with the boreholes spaced 10 m apart, is shown to increase annual energy usage by as much as 1.9% after 20 years of operation. The increase in energy consumption is due mostly to the heat pump's lower performance resulting in additional compressor energy. The heat pump's lower capacity results in more electricity consumption by the supplementary immersion heater. For a system with the neighboring borehole located at a distance of 20 m, the neighboring system effects cause an increase of about 1% after 20 years of operation.

The analysis of the effect of neighboring systems described is preliminary in nature. Several improvements should be made, and additional cases simulated to further characterize the neighboring system effects. These are:

- Pumping energy is neglected but should be considered in future studies. For heating-dominated applications, the pumping energy helps reduce the decline in the heat pump inlet temperature. This effect should be small with a properly designed system, but its effect should be quantified.
- Future studies should better consider the effect of all systems on each other, such as the effect of the lone system on the neighboring system instead of simply prescribing ground loads for this system.
- Additional cases should be considered, such as different starting years for neighboring systems and multiple neighboring systems. It would also be of interest to determine the additional borehole depth that would be required to mitigate the effect of neighboring systems.

Beyond, the effect of neighboring systems, the cross g-functions have other possible applications, which should be further explored. These include adding to a ground heat exchanger after the system has operated for some time and zone of the ground heat exchanger so that some parts are operated at different times of the year.

NOMENCLATURE

α – Thermal diffusivity (m^2/s)

d – Distance (m)

D – Borehole depth (m)

g – g-function (-)

H – Borehole active length (m)

k – Thermal conductivity (W/m-K)

N_b – Number, boreholes

q – Normalized heat load (W/m)

r_b – Borehole radius (m)

t – Time (s)

t_S – Time scale (s)

T_w – Borehole wall temperature (°C)

u – Point location

x, y, z – Cartesian coordinates (m)

x', y', z' – Mirrored Cartesian coordinates (m)

X_b—Borehole spacing (m)

REFERENCES

BLOCON (2017). Earth Energy Designer (EED) Version 4 Update Manual.

Cimmino, M. (2018). "Fast calculation of the g-functions of geothermal borehole fields using similarities in the evaluation of the finite line source solution." *Journal of Building Performance Simulation* **11**(6): 655-668.

Cimmino, M. and M. Bernier (2014). "A Semi-analytical Method to Generate g-functions for Geothermal Bore Fields." *International Journal of Heat and Mass Transfer* **70**: 641-650.

Claesson, J. and P. Eskilson (1985). Thermal analysis of heat extraction boreholes. *Enerstock 85 (the 3rd International Conference on Energy Storage for Building Heating and Cooling)*, Toronto, Canada. 222-227.

Eskilson, P. (1987). Thermal Analysis of Heat Extraction Boreholes, University of Lund.

Eskilson, P. and J. Claesson (1988). "Simulation Model for Thermally Interacting Heat Extraction Boreholes." *Numerical Heat Transfer* **13**: 149-165.

Fascì, M. L. and A. Lazzarotto (2019). A novel model for the estimation of thermal influence of neighboring borehole heat exchangers. *European Geothermal Congress*, The Hague, The Netherlands. June 11-14. 1-6.

Fascì, M. L., A. Lazzarotto, J. Acuña and J. Claesson (2018). Thermal influence of neighboring GSHP installations: relevance of heat load temporal resolution. *IGSHPA Research Conference*, Stockholm, Sweden.

Fisher, D. E., S. J. Rees, S. K. Padhmanabhan and A. Murugappan (2006). "Implementation and validation of ground-source heat pump system models in an integrated building and system simulation environment." *HVAC&R Research* **12**(3a): 693-710.

Gehlin, S. E. A. and J. D. Spitler (2014). Design of residential ground source heat pump systems for heating dominated climates - trade-offs between ground heat exchanger design and supplementary electric resistance heating. *ASHRAE Winter Conference*, New York, NY, ASHRAE.

Gustafsson, A.-M. and S. E. A. Gehlin (2008). "Influence of natural convection in water-filled boreholes for GCHP." *ASHRAE Transactions* **114**(1): 416--423.

Marcotte, D. and P. Pasquier (2009). "The Effect of Borehole Inclination on Fluid and Ground Temperature for GLHE Systems." *Geothermics* **38**(4): 392-398.

Mitchell, M. S. (2019). An enhanced vertical ground heat exchanger model for whole-building energy simulation. Ph.D., Oklahoma State Univesity. Stillwater, OK.

Moin, P. (2010). Fundamentals of Engineering Numerical Analysis. New York, NY, Cambridge University Press.

Nordman, R. (2014). Research Institutes of Sweden. Personal communication with S. Gehlin. Sept. 1, 2014.

Spitler, J. D. (2000). GLHEPro -- A Design Tool for Commercial Building Ground Loop Heat Exchangers. *4th International Heat Pump in Cold Climates Conference*, Aylmer, Québec. Aug. 17-18.

Spitler, J. D. and M. A. Bernier (2016). Vertical borehole ground heat exchanger design methods. Advances in Ground-Source Heat Pump Systems. S. J. Rees. Amsterdam, Woodhead Publishing**:** 29-61.

Spitler, J. D., M. D. Wong and S. E. A. Gehlin (2014). Effect of residential ground source heat pump system design on CO2 emissions in Sweden. *ASHRAE Annual Conference*, Seattle, WA. June 28--July 2.

Witte, H. J. L. (2018). A novel tool for assessing negative temperature interactions between neighboring borehole heat exchanger systems. *14th International Conference on Energy Storage-EnerSTOCK2018*, Adana, Turkey. April 25-28. 1-14.

Yavuzturk, C. and J. D. Spitler (1999). "A Short Time Step Response Factor Model for Vertical Ground Loop Heat Exchangers." *ASHRAE Transactions* **105**(2): 475-485.

Yu, M., H. Rang, J. Zhao, K. Zhang and Z. Fang (2017). Influence of Ground Heat Exchanger Zoning Operation on the GSHP System Long-term Operation Performance. *IGSHPA Technical/Research Conference Proceedings*, Denver, CO. 144-151.